Vol. 02, Iss. 1 (2024) 1-19, DOI: 10.61552/JME.2024.01.001

JME

Journal of Materials and Engineering

www.jme.aspur.rs

Research article

Mathematical Models for Adsorption Capacity and Percent Removal of Heavy Metals from Water Using Stat-Ease 360

Abdulhalim Musa Abubakar[a], Eva Schieferstein[b], Irnis Azura Zakarya[c,*], Baudilio Coto[d], Chantawan Noisri[e], Adegoke Taiwo Mobolaji[f], Hijaz Ahmad[g]

[a]*Department of Chemical Engineering, Faculty of Engineering, Modibbo Adama University, P.M.B 2076, Yola, Adamawa State, Nigeria,*
[b]*Fraunhofer UMSICHT, Osterfelder Str. 3, D-46047 Oberhausen, Germany,*
[c]*Sustainable Environment Research Group (SERG), Centre of Excellence Geopolymer and Green Technologies (CEGeoGTech), Universiti Malaysia Perlis, 02600 Arau, Perlis, Malaysia,*
[d]*Chemical, Energy and Mechanical Technology Department, School of Experimental Sciences and Technology (ESCET), Rey Juan Carlos University, c/ Tulipan s/n, 28933 Móstoles, Madrid, Spain,*
[e]*Department of Mathematics and Statistics, Faculty of Science, Thaksin University, Phatthalung, Thailand,*
[f]*Department of Mathematics and Statistics, First Technical University, Km 15 Lagos - Ibadan Expy, 200261, Ibadan, Oyo State, Nigeria,*
[g]*Section of Mathematics, International Telematics University Uninettuno, Corso Vittorio Emanuele II, 39, 00186, Roma, Italy.*

Keywords:

Heavy metals
Adsorbent
Watermelon rind
Water treatment
Ngomari
Blanksheet design
Stat-Ease 360
Adsorption capacity

* Corresponding author:

Irnis Azura Zakarya
E-mail: irnis@unimap.edu.my

Received: 8 September 2023
Revised: 10 October 2023
Accepted: 12 November 2023

A B S T R A C T

Heavy metal removal using adsorbent materials like watermelon rind, as investigated herein, will ensure a safe drinking water for consumption. For the first time, mathematical models taking A = adsorbent dosage, B = contact time and C = initial concentration as input variables were developed using Stat-Ease 360 design of experiment (DOE) tool for adsorption capacity (R1) and percent removal of heavy metals including, arsenic, cadmium, chromium, copper and lead (R2) in water, as two sole output variables. The models generated based on existing experimental observations (A, B, C) can be used to predict the responses or outputs of the adsorption process, especially looking at their respective satisfactory statistical performance parameters obtained. Several 3D surface and contour plots reveal the optimal factor combination for peak response performance for a particular metallic contaminant in the water. Optimal values for arsenic removal are 0.1g A, 120 min B, 3.12 mg/g R1 and 100% R2. Those of other metals present are as follows: 0.1g A, 60 min B, 0.17 mg/L C, 144.75 mg/g R1 and 85.78% R2 for cadmium; 0.1-1.2g A, 0<B≤120 min, 0.028 mg/L C, 215 mg/g R1 and 85.53% R2 for chromium; 0.1-1.2g A, 0<B≤120 min, 0.041 mg/L C, 275 mg/g R1 and 80% R2 for copper and; 0.1-1.2g A, 0<B≤120 min, 0.029 mg/L C, 205 mg/g R1 and 83.42% R2 for lead. This study falls short of many heavy metals such as zinc, nickel, cobalt, antimony, iron and mercury removal used to test the effect of other factors like pH, presence of co-existing ions, temperature and sorbent particle size for their adsorption performance.

1. INTRODUCTION

Heavy metal poisoning of natural water sources is a developing problem due to its negative impact on both human health and the environment [1–3]. Heavy metals are characterized as having a specific gravity > 5g/cm^3; e.g., zinc (Zn), iron (Fe), copper (Cu), chromium (Cr), mercury (Hg), lead (Pb), nickel (Ni), cobalt (Co), cadmium (Cd), arsenic (As), antimony (Sb) etc. [4]. Heavy metals, such as Pb, Cd, and Hg [5–7], are hazardous and persistent contaminants that can accumulate in aquatic environments, posing a major danger to biodiversity and water quality [8]. To address this important issue, the development of efficient and cost-effective water treatment technology is critical. Adsorption has emerged as a promising method for the removal of heavy metals from aqueous solutions. It involves the attachment of metal ions to the surface of solid adsorbents [9], [10], rendering them less soluble and, therefore, more easily separable from water. The success of adsorption processes depends on several factors, including the choice of adsorbent material, operating conditions, and the mathematical models used to describe the adsorption behavior. Adsorbent materials reported in the literature for heavy metal removal from water are becoming countless. Examples are clinoptilolite [11], polymer immobilized biomass [2, 12], biochar [13], plant waste [14, 15], bentonite [16], zeolite [5], activated carbon [4, 17], activated sludge [18] and microbes [19], to mention a few. This research endeavors to contribute to the field of heavy metal removal through adsorption by employing Stat-Ease 360, a powerful statistical software tool widely recognized for its effectiveness in the design and analysis of experiments. The primary objectives of this study are threefold: (1) to develop mathematical models that accurately describe the adsorption capacity of selected adsorbent materials, (2) to establish models predicting the percentage removal of heavy metals from contaminated water and (3) to hunt for optimal choice of factors for maximum yield of the responses mentioned in 1 & 2 from a 3D surface plot. Principally, every optimization process take in 3 key steps [20]: (a) accomplishing the statistically designed experiments, (b) approximating the coefficients in a mathematical model, and (c) predicting the response and scrutinizing the adequacy of the model.

In pursuit of these objectives, we will conduct a series of controlled experiments, systematically varying the influential factors such as contact time, adsorbent dosage, and initial metal ion concentration, as exemplified in previously related study using banana stalk biosorbent demonstrated using central composite design (CCD) response surface methodology (RSM) [21]. Temperature and pH as tested on zinc, cadmium, chromium and nickel removal from water by Adamu (2023), are additional factors affecting the process. In addition, natural water embraces several competitive ions that might contend with the adsorbate for a few numbers of active sorption sites, upsetting the sorption capacity of the biosorbent. The presence of competitive ions may surge or lessen the biosorption capacity of biosorbent because of the boosted number of surface binding sites ensuing from parallel ion sorption or competing processes on surface binding sites of biosorbent, as reported by Poudel (2022). The data generated will be analyzed using Stat-Ease 360, allowing us to derive empirical models that elucidate the relationships between the adsorption process variables and the response variables of adsorption capacity and percent removal. What differentiates this work with the one done by Atta et al. (2022) is the use of a user-define blank sheet design (BSD), the use of watermelon rind data instead of rice husk, and the non-use of adsorption isotherm kinetic models [17] to correlate the empirical data. This research will not only address the need for more effective heavy metal removal methods but also contributes to the understanding of the underlying mechanisms of adsorption. The mathematical models developed herein are expected to provide valuable insights into the optimization of adsorption processes, thereby enhancing their efficiency and sustainability. As the world grapples with the ever-increasing challenges of water pollution and environmental degradation, the outcomes of this study have the potential to inform the design and implementation of advanced water treatment systems, ultimately safeguarding the health of ecosystems and human populations alike. Because the presence of heavy metals in water are inevitable as they are introduced in aquatic environments by weathering, volcanic processes, atmospheric deposition and erosion of the geological environment or through anthropogenic source [4, 13, 22,23].

2. METHODOLOGY

2.1 Biosorption Constraints

Based on an existing experimental observation obtained from the adsorption of heavy metals from water at Ngomari Bus Stop, Maiduguri, Nigeria using watermelon rind, where A represents adsorbent dosage, B, contact time and C, concentration of the heavy metals in water, the foregone parameters was linked mathematically to the adsorption capacity (R1) and percentage removal of heavy metal (R2), called responses respectively. In this case, Stat-Ease 360 was employed to assess the existing parameter values corresponding with the experimentally obtained R1 and R2 and help suggest the best 3-variable numerical model that fits R1 and R2 output variables. Factors A, B and C corresponding with R1 and R2 for each heavy metal, namely, arsenic (As), cadmium (Cd), chromium (Cr), copper (Cu) and lead (Pb), present in the water were thus defined separately in Stat-Ease 360 software. In essence, basic mathematical model satisfying R1 and R2 of each individual metallic element present was expected. This is a total of 10 mathematical models for the 5 metallic components of the Ngomari water.

2.2 Stat-Ease 360 Blank Sheet Design

Blank Spreadsheet Design (BSD) was selected following the steps: Custom Designs ⟶ Blank Spreadsheet. Under BSD, number of numeric factors and rows were set to 3 and 13 respectively, with 0 categoric factors defined. BSD was chosen so as to import the existing data to the design sheet. Their units as well as the lower and upper values were registered accordingly. Next, 2 responses (R1 & R2) with their respective units were entered. Stat-Ease 360 was observed to generate possible factors A, B and C values with their R1's or R2's in separate specification. Since the goal is to model the responses, these new possibilities were ignored. Also expected in this kind of design are the Analysis of Variance (ANOVA) for the best model, fit statistics, model equations and 3D surface plots. This study examined the work carried out by Kumar et al. (2018) on Cd and Pb ions adsorption using RSM-CCD for possible replication on multiple heavy metal presence in Ngomari tap water using BSD in a Design of Experiments (DOE) software.

2.3 Model Comparison

Using the number of parameters or predictors in a model (k) and the sample size (n), both the Bayesian Information Criterion (BIC) and Corrected Akaike Information Criterion (AICc) given in Equations 1 and 2 respectively [24], the best model was chosen.

$$\mathrm{BIC} = -2\ \mathrm{Log\ Likelihood} + \mathrm{k}\ln(\mathrm{n}) \quad (1)$$

$$\mathrm{AICc} = -2\ \mathrm{Log\ Likelihood} + 2\mathrm{k} + \frac{2\mathrm{k}(\mathrm{k}+1)}{\mathrm{n}-\mathrm{k}-1} \quad (2)$$

Calculating BIC and AICc relies on the values of the -2 Log Likelihood obtained from Stat-Ease 360.

3. RESULTS AND DISCUSSION

3.1. Predicted Responses Using Proposed Equations

Linear models according to Stat-Ease 360 proposal, best correlates the observed R1 and R2 for As. The respective R1 and R2 numerical models were given in terms of the actual and coded factors (Figures 1-5). Factor coding is a technique used to represent categorical or numerical variables in a standardized way so that they can be used in statistical models or analyses. By "coded", it means that the variables have been transformed into a common scale or format to make them comparable and suitable for statistical analysis [25]. For example, in DOE, factors may be coded to simplify the interpretation of results and to ensure that the factors have the same units or scale. This coding process allows researchers to analyze and compare the effects of different factors on an outcome [26]. The coefficient estimate (Figures 1-5) represents the expected change in response per unit change in factor value when all remaining factors are held constant.

				R = Response							
				Expt.	Expt.	Corr.	Corr.				
	Factor A	Factor B	Factor C	R1	R2	R1	R2				
Runs	**Adsorbent Dosage (g)**	**Contact Time (min)**	**Concentration (mg/L)**	**Adsorption capacity, (mg/g)**	**% Removal**			LINEAR EQUATION			
									Actual		**Coded**
0	0	0	0.004	0	0	-2.48E-06	0.00	R1 =		R1 =	
1	1.2	20	0	0.33	100	-0.883938	100.00	2.91103		-0.2213	
2	1.2	120	0	0.33	100	-0.442538	100.00	-3.23604	A	-1.94	A
3	0.65	70	0	0.62	100	1.116584	100.00	0.004414	B	0.2649	B
4	0.65	120	0	0.62	100	1.337284	100.00	-727.75812	C	-1.46	C
5	0.65	70	0	0.62	100	1.116584	100.00				
6	0.65	70	0	0.62	100	1.116584	100.00	LINEAR EQUATION			
7	0.65	70	0	0.62	100	1.116584	100.00		**Actual**		**Coded**
8	0.65	70	0	0.62	100	1.116584	100.00	R2 =		R2 =	
9	0.65	20	0	0.62	100	0.895884	100.00	100		50	
10	0.65	70	0	0.62	100	1.116584	100.00	-2.2683E-14	A	0	A
11	0.1	120	0	4	100	3.117106	100.00	-5.08E-17	B	0	B
12	0.1	70	0	4	100	2.896406	100.00	-25000.00000	C	-50	C
13	0.1	20	0	4	100	2.675706	100.00				

Fig. 1. R1 and R2 Model Coefficients, Type and Correlated Values for Arsenic Biosorption.

				R = Response						
				Expt.	Expt.	Corr.	Corr.	QUADRATIC EQUATION		
	Factor A	Factor B	Factor C	R1	R2	R1	R2		**Actual**	**Coded**	
Runs	**Adsorbent Dosage (g)**	**Contact Time (min)**	**Concentration (mg/L)**	**Adsorption capacity, (mg/g)**	**% Removal**			R1 =	198.5815	13.44	
									-356.838	-39.43	A
0	0	0	0.17	0	0	-3.738E-06	-0.22584		0.212302	7.11	B
1	0.65	70	0.128	6.46	24	6.46369133	24.18986		-1156.61	-18.36	C
2	0.65	120	0.123	7.23	27	7.22730142	27.20637		-0.18428	-6.63	AB
3	0.65	70	0.103	10.3	39	10.411934	38.91041		1138.695	49.87	AC
4	0.1	20	0.098	72	42	71.9999172	42.13427		3.9168	17.16	BC
5	0.65	70	0.091	12.5	46	12.2770249	45.97627		159.7647	57.52	A^2
6	1.2	120	0.077	7.75	54	7.74730298	53.94003		-0.00303	-10.89	B^2
7	0.65	70	0.069	15.54	59	15.645707	58.93036		-67.7154	-0.3609	C^2
8	0.1	120	0.061	109	64	108.997277	64.06548	LINEAR EQUATION			
9	0.65	70	0.051	18.31	70	18.3531463	69.52915	R2 =			
10	0.65	20	0.046	19.08	72	19.0799156	72.40086		99.87389	42.46	
11	1.2	20	0.041	10.75	75	10.7499133	74.99282		-0.64028	-0.3842	A
12	0.65	70	0.035	20.77	79	20.7229219	78.9503		0.001448	0.0869	B
13	0.1	70	0.024	146	85	144.754393	85.7795		-588.822	-42.98	C

Fig. 2. R1 and R2 Model Type, Coefficients and Correlated Values for Cadmium Biosorption.

				R = Response						
				Expt.	Expt.	Corr.	Corr.	QUADRATIC EQUATION		
	Factor A	Factor B	Factor C	R1	R2	R1	R2		**Actual**	**Coded**	
Runs	**Adsorbent Dosage (g)**	**Contact Time (min)**	**Concentration (mg/L)**	**Adsorption capacity, (mg/g)**	**% Removal**			R1 =	238.5035	14.39	
									-440.482	-44.44	A
0	0	0	0.199	0	0	-4.61327E-06	-0.39353		0.189892	13.97	B
1	0.65	70	0.118	12.46	40	12.46337624	40.03163		-1198.37	-21.73	C
2	0.65	120	0.109	13.85	45	13.85512646	44.57599		-0.15812	-5.69	AB
3	0.65	70	0.091	16.62	51	16.6187739	53.60126		1142.265	58.6	AC
4	0.1	20	0.087	112	56	112.0001314	55.85555		4.3163	22.14	BC
5	0.65	70	0.083	17.85	58	17.8498038	57.62189		205.2179	73.88	A^2
6	1.2	120	0.069	10.83	65	10.83513369	64.41402		-0.00293	-10.56	B^2
7	0.65	70	0.061	21.23	69	21.23466683	68.67862		-0.71087	-0.0052	C^2
8	0.1	120	0.055	144	72	144.0051129	71.98037	LINEAR EQUATION			
9	0.65	70	0.048	23.23	75	23.23448972	75.21215	R2 =			
10	0.65	20	0.041	24.31	79	24.31013541	78.70905		99.61965	42.31	
11	1.2	20	0.036	13.58	81	13.58014261	80.95682		-0.48205	-0.2892	A
12	0.65	70	0.031	25.85	84	25.84928019	83.75599		0.000423	0.0254	B
13	0.1	70	0.028	171	85	172.4199123	85.52885		-502.579	-42.97	C

Fig. 3. R1 and R2 Model Type, Coefficients and Correlated Values for Chromium Biosorption.

				R = Response							
				Expt.	Expt.	Corr.	Corr.		QUADRATIC EQUATION		
	Factor A	Factor B	Factor C	R1	R2	R1	R2			Actual	Coded	
Runs	Adsorbent Dosage (g)	Contact Time (min)	Concentration (mg/L)	Adsorption capacity, (mg/g)	% Removal				R1 =	336.6628	22.39	
										-604.809	-65.84	A
0	0	0	0.286	0	0	1.98276E-06	-0.15285			0.3641	11.56	B
1	0.65	70	0.22	10.15	23	10.14736982	22.7977			-1176.33	-30.63	C
2	0.65	120	0.208	12	27	12.00276093	27.11968			-0.33399	-12.02	AB
3	0.1	20	0.158	128	44	128.0000774	44.32948			1166.611	85.75	AC
4	0.65	70	0.152	20.61	46	20.61888435	46.41117			3.7871	27.84	BC
5	0.65	70	0.15	20.92	47	20.9264723	47.10568			270.311	97.31	A^2
6	1.2	120	0.13	13	54	13.00279177	54.04896			-0.00492	-17.71	B^2
7	0.65	70	0.117	26	59	25.99839198	58.56516			-2.84119	-0.0426	C^2
8	0.1	120	0.097	189	66	189.002761	65.82195		LINEAR EQUATION			
9	0.65	70	0.087	30.62	69	30.6038582	68.98286		R2 =			
10	0.65	20	0.078	32	72	32.00008331	71.95328			99.16261	42.4	
11	1.2	20	0.069	18.08	75	18.08008646	74.92183			-0.28501	-0.171	A
12	0.65	70	0.055	35.5	80	35.51071859	80.09508			0.003098	0.1859	B
13	0.1	70	0.041	245	85	245.3487815	85.11344			-347.257	-42.54	C

Fig. 4. R1 and R2 Model Coefficients, Type and Correlated Values for Copper Biosorption.

				R = Response								
				Expt.	Expt.	Corr.	Corr.					
	Factor A	Factor B	Factor C	R1	R2	R1	R2		QUADRATIC EQUATION			
Runs	Adsorbent Dosage (g)	Contact Time (min)	Concentration (mg/L)	Adsorption capacity, (mg/g)	% Removal			R1 =		R2 =		
								Actual	Coded	Actual	Coded	
0	0	0	0.201	0	0	2.55527E-06	4.28244E-06	236.259	15.75	96.2739	42.52	
1	0.65	70	0.157	6.77	21	6.770424967	20.98608532	-423.061	-46.22	5.14586	-0.0917	A
2	0.65	120	0.148	8.15	26	8.150983463	26.00363384	0.2506	7.98	-0.01355	-0.2377	B
3	0.1	20	0.116	85	42	85.00002505	42.00010206	-1175.65	-21.53	-448.299	-43.29	C
4	0.65	70	0.104	14.92	48	14.92129341	48.03494832	-0.22563	-8.12	-0.00599	-0.2157	AB
5	0.65	70	0.094	16.46	53	16.45992849	53.04236083	1154.014	59.55	-22.178	-1.14	AC
6	1.2	120	0.092	9.08	54	9.080975805	54.0036318	3.87784	20.01	-0.11155	-0.5756	BC
7	0.65	70	0.082	18.31	59	18.30659875	59.01096587	189.0485	68.06	-1.99052	-0.7166	A^2
8	0.1	120	0.072	129	64	129.0010201	64.00363171	-0.00357	-12.85	0.000217	0.7803	B^2
9	0.65	70	0.062	21.38	69	21.38512957	68.86096825	1.16727	0.0086	-152.614	-1.13	C^2
10	0.65	20	0.056	22.31	72	22.31002392	72.00010245					
11	1.2	20	0.048	12.75	76	12.750018	76.0001029					
12	0.65	70	0.041	24.62	79	24.61859196	79.07207048					
13	0.1	70	0.029	172	85	171.4483892	83.42184883					

Fig. 5. R1 & R2 Correlated Values, Generated Model Type and their Coefficients for Lead Biosorption.

In extension, the main reason for choosing the R1 linear model for As (Figure 1) above all other model types is because its sequential p-values is 0.0089 < 0.05, indicating the presence of significant model terms (i.e., A & C) – burrowing Fanaie et al. (2016) RSD + predictive model analysis. But when a p-value of a linear model is null, it typically implies that none of the predictor variables included in the model are statistically significant in explaining the variation in the response variable (e.g., R2 from As). In other words, none of the predictor variables (A, B & C) have significant linear relationship with the response variable. For Cd, the model fitting the 3 factors are quadratic for R1 and linear equation for R2 output variable, as shown in Figure 2. Where the experimental R values are very close to the correlated or predicted R(s) using the respective model equations. Under Cd-R1, Stat-Ease 360 suggests both linear and quadratic model source. The choice of the quadratic model for Cd-R1 in this work was because it has a p-value < 0.0001 lower than the linear model with a value of 0.0093. Notwithstanding, both models are suitable as their sequential p-values are < 0.05. Hence, in the selected quadratic model for Cd-R1, A, B, C, AB, AC, BC, A^2 and B^2 are significant model terms. As for Cd-R2, where a linear model is most suited for representing the outcome, A & C are significant model terms as its p-value is also < 0.0001.

Similar R1 and R2 model types (seen in Figure 2) were obtained in Figures 3 and 4 for Cr and Cu DOE analysis, respectively. Again, linear and quadratic models predict the responses under Cr-R1 satisfactorily, but the quadratic model was chosen in this study due to its low p-value (< 0.0001 – as shown in Figure 3). Cr-R2 linear model has the same p-value as above. Likewise, A,

B, C, AB, AC, BC, A^2 and B^2 are significant model terms of R1 quadratic equation, while C is the only significant model term for R2 linear equation for Cr % removal [20]. Cu-R1 quadratic and Cu-R2 linear models shown in Figure 4, both have p-values < 0.0001 and their respective significant terms are similar to those of Figure 3 equations. P-values of < 0.0001 and 0.0346 for Pb-R1 and Pb-R2 quadratic models was a sufficient criterion favouring the choice of the given model equation shown in Figure 5, having similar significant model terms compared to all quadratic models under Cd, Cr and Cu.

3.2. Fit Statistics and Model Selection Criteria

Adequate Precision measures the signal to noise ratio, where a ratio > 4 is desirable according to Ogunleye et al. (2015). In this analysis, the Adeq. Precision ranges from 8.7342-46499.8 under all the response model equations, except under As-R2. This signifies an adequate signal and that the models under such constrain can be used to navigate the design space. Values in Table 1 showcased the statistical results of the highest order polynomial whose additional terms are significant and the model is not aliased.

Table 1. Predicted Model Statistical Performance.

	Arsenic		**Cadmium**		**Chromium**	
	R1	**R2**	**R1**	**R2**	**R1**	**R2**
Std. Dev.	0.8258	0.0000	0.1607	0.2481	0.0035	0.9371
Mean	1.05	92.31	23.82	50.08	33.52	59.62
C.V. %	78.82	0.0000	0.6747	0.4954	0.0105	1.57
R^2	0.7080	1.0000	1.0000	0.9999	1.0000	0.9987
Adjusted R^2	0.6107	1.0000	1.0000	0.9999	1.0000	0.9983
Predicted R^2	NA(1)	NA(1)	NA(1)	0.9998	NA(1)	0.9979
Adeq. Precision	8.7342	NA(1)	773.1913	575.3608	46499.7517	161.8778
PRESS	NA(1)	NA(1)	NA(1)	1.26	NA(1)	12.95
-2 Log Likelihood	27.14	-	-29.70	-4.13	-128.97	30.42
BIC	37.40	-	-4.05	6.13	-103.32	40.68
AICc	40.14	-	100.30	8.87	1.03	43.42
Lack of Fit	6.14	0.0000	0.0000	0.0000	0.0000	0.0000
	Copper		**Lead**			
	R1	**R2**	**R1**	**R2**		
Std. Dev.	0.0129	0.2600	0.0037	0.0963		
Mean	41.22	50.92	28.37	51.00		
C.V. %	0.0313	0.5105	0.0130	0.1889		
R^2	1.0000	0.9999	1.0000	1.0000		
Adjusted R^2	1.0000	0.9999	1.0000	1.0000		
Predicted R^2	NA(1)	0.9998	NA(1)	NA(1)		
Adeq. Precision	16685.93	556.5043	39748.6227	935.7903		
PRESS	NA(1)	1.25	NA(1)	NA(1)		
-2 Log Likelihood	-95.25	-2.92	-127.75	-43.01		
BIC	-69.60	7.34	-102.10	-17.36		
AICc	34.75	10.08	2.25	86.99		
Lack of Fit	0.0000	0.0000	0.0000			

(1) Case(s) with leverage of 1.0000: Pred R^2 and PRESS statistic not defined.
Thus, NA stands for Not Available

It is advisable to always focus on the model maximizing the adjusted R^2 and the predicted R^2. Therefore, the predicted R^2 's' of 0.9998, 0.9979 and 0.9998 under Cd-R2, Cr-R2 and Cu-R2 are in reasonable agreement with their corresponding adjusted R^2 values of 0.9999,

0.9983 and 0.9999, with the respective difference of 0.0001, 0.0004 and 0.0001 less than 0.2 [22]. Predicted R^2 's' that are not available or undefined may be due to low-quality or noisy data, leading to poor model predictions and, consequently, an undefined predicted R^2. It may also imply that the software couldn't calculate a meaningful value for the predicted R^2 based on the model specified. The later could be true for this analysis, as the values are normally computed based on the residual variance in the models. It must not be forgotten that the predicted R^2 measures how well the statistical model predicts new, unseen data. Note that, if the response variable doesn't vary much in the dataset, it can be challenging to create a predictive model, and the predicted R^2 may not be meaningful.

In Stat-Ease 360 and other statistical software, "C.V. %" typically stands for "Coefficient of Variation Percentage". C.V. % is a statistical measure that expresses the relative variability of a dataset. It is calculated as the ratio of the standard deviation to the mean of a dataset, multiplied by 100 to express it as a percentage. A low percentage indicates that the data points in your dataset are relatively close to the mean, suggesting low variability or dispersion in the data [21]. A high percentage indicates that the data points are spread out more widely from the mean, indicating higher variability or dispersion in the data. High C.V.% > 50%, especially under As-R1, suggests a high degree of variability among the data points. Other C.V.% in the range of 0.0105-1.57 or < 10%, as shown in Table 1, suggests a tightly clustered data points around the mean. If the C.V.% is moderate or between 10-50%, it points to a moderate level of variability. But if C.V.% is zero as in As-R2, it shows that the Std. Dev is also zero at constant mean (92.31). Such scenario demonstrates an identical data point in the dataset having no variability or spread. In other words, all data points have exactly the same value (see Figure 1 – Expt. R2 column), are highly uniform, incredibly stable and lacks diversity; and analysts will be incapable of instigating a meaningful conclusion from the data.

PRESS stands for 'Predicted Residual Error Sum of Squares', used to evaluate the predictive performance of a statistical model, particularly in the context of regression analysis or DOE. Just like the predicted R^2, PRESS is used to estimate how well a statistical model is likely to perform on new, unseen data. There is no specific typical range for PRESS values. Lower PRESS values indicate that the model is better at predicting new observations, while higher PRESS values suggest that the model may have difficulty making accurate predictions on new data. Zero lack-of-fit is in line with R^2 values that is $\cong 1$ or unity in the selected models. The lack-of-fit of 6.14 existing under As-R1 in Table 1, proves the existence of unexplained variation in the model. In general, smaller lack-of-fit statistic portrays a better fit between the model and the data, while a larger value suggests that the model may not fit the data well. Equal R^2 and adjusted R^2 advocates model not overfitting or underfitting and a balance between model complexity and model fit has been found. There is no need to add or remove predictors for improved model performance. Stat-Ease 360 used the estimated -2 Log Likelihood, BIC, and AICc values shown in Table 1 to choose the best-fitting model among different candidate models before suggesting the models displayed in Figures 1-5.

3.3. Optimal Responses and Fit Analysis

Dual factor combined 3D plots with response R1 and R2 for As, Cd, Cr, Cu and Pb metals present in the Ngomari Bus Stop water are depicted in Figures 6-15 (a-c). Predicted against empirical R1 and R2 relationships are also shown in Figures (6-15)d.

3.3.1. Arsenic

Figure 6a suggests that for a given adsorbent and water conditions, the most efficient removal of As from water occurs when 0.1g of the adsorbent per gram of water is used and allowed to come into contact with the water for 120 min. During this time, the adsorbent can effectively remove As from water. The adsorbent has a maximum capacity of 3.12 mg of As per gram of adsorbent (mg/g). The statement indicates that these conditions represent an optimized process for As removal. Having a negative value (-0.44 mg/g) for optimal adsorption capacity in Figure 6b makes no physical sense. This corresponds with 0 mg/L initial concentration of As in water

for 1.2 g adsorbent dosage. Though this is desirable as it is well below 0.7 mg/L WHO standard for As in water [23]; because if there is no As in the water, then there should be nothing to absorb. An ineffective adsorption occurs in Figure 6c, if 20 minutes contact time matched with 0 mg/L corresponds with optimal adsorption capacity of -0.8839 mg/g.

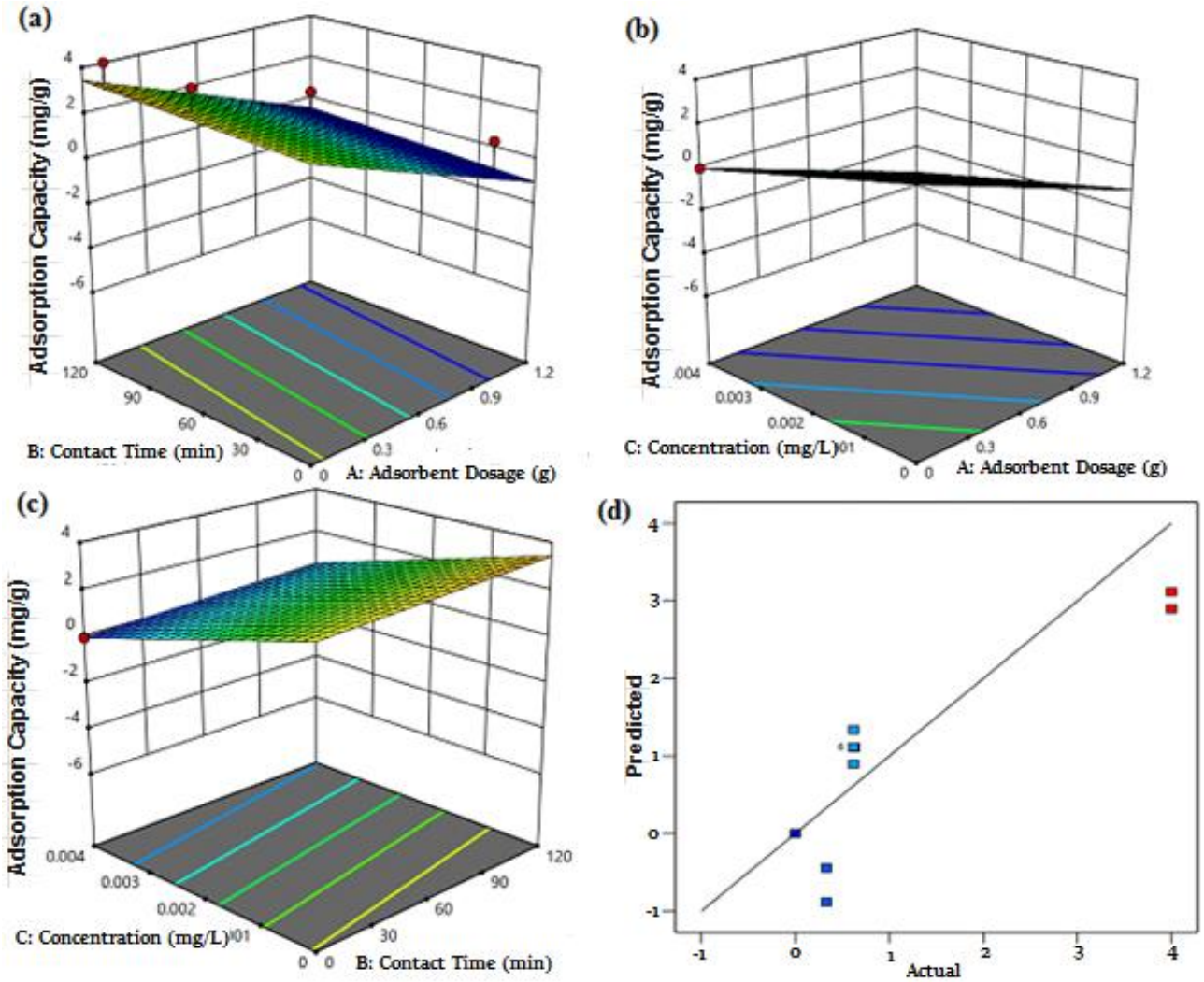

Fig. 6. R1 Versus A-B, A-C & B-C and its Observed-Predicted Values Fit.

Optimum % removal of As equivalent to 100% show that the treatment process using specified adsorbent and conditions, can completely remove As from water. The water that has undergone this treatment as observed in Figure 7a should be As free. This is a desirable outcome, especially when dealing with toxic contaminants like As in water. Tallied with a longer contact time (120 min) and 1.2g adsorbent dosage, it demonstrates that thorough As removal requires a more extended exposure to the treatment process and a relatively larger quantity of adsorbent. Within a dosage range from 0.1-1.2g, the treatment process consistently achieves complete As removal based on the 100% removal shown in Figure 7b. Implication of having an initial concentration of 0 mg/L is that no As was present in the water at the beginning, which is an idealized scenario. In reality, water sources may have some level of As contamination, so achieving complete removal may not be as straightforward. It is obvious that the treatment process is exceptionally efficient at removing As, achieving a 100% removal rate, requiring an extended duration of 120 min under an idealized 0 mg/L initial concentration condition, in accordance with Figure 7c. Visceral cancer and skin issues are harmful effects of exposure to As beyond the maximum contaminant level (MCL) of 0.05 mg/L [4].

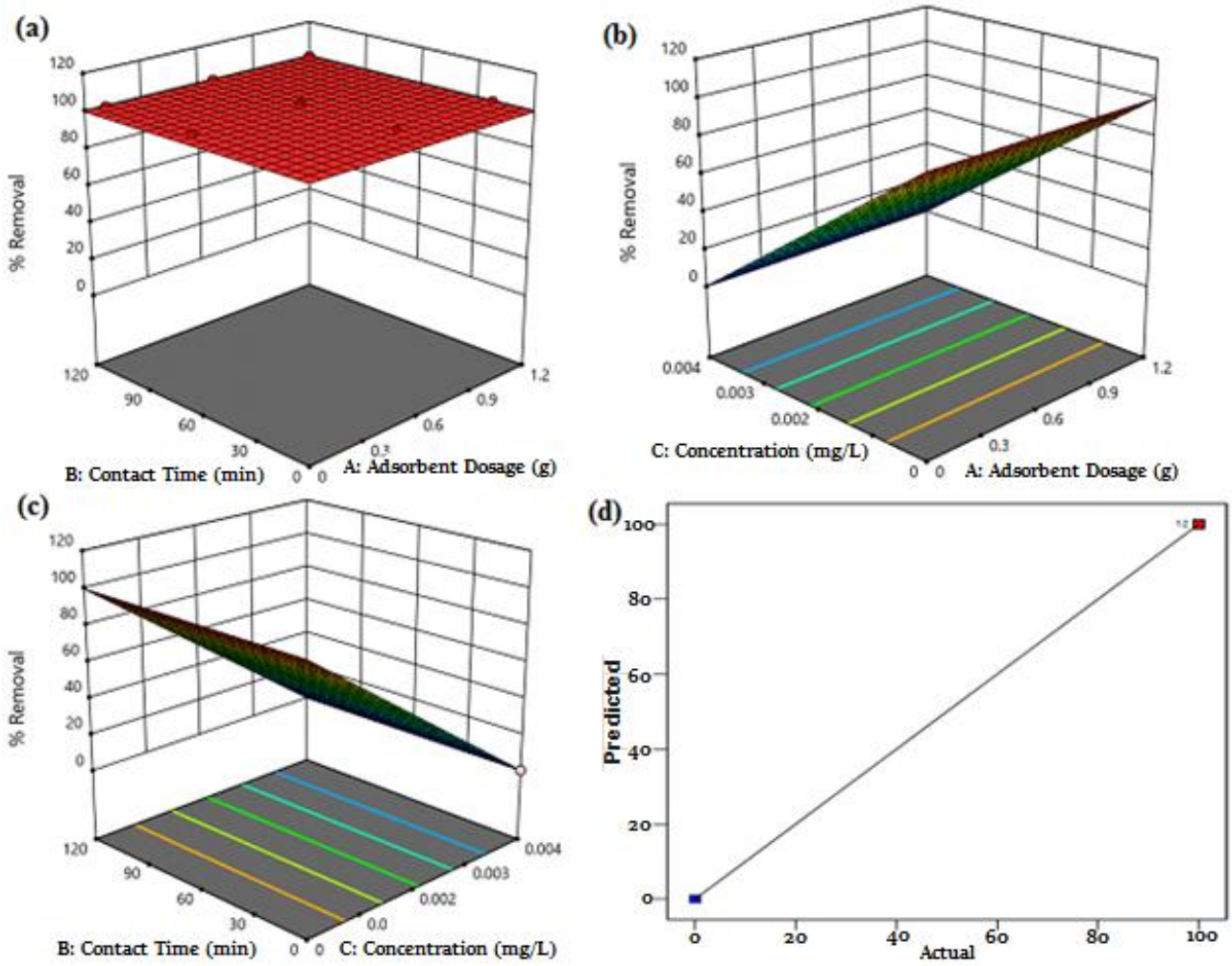

Fig. 7. R2 Versus A-B, A-C & B-C and its Observed-Predicted Values Fit.

3.3.2. Cadmium

Upward curved surface in the 3D plot observed moving along the axes signifies that as both independent variables (A-B & A-C) in Figures 8(a-b) are increased, the dependent variable (R1) for Cd removal tends to increase. By implication, there is a positive correlation between the independent variables and the dependent variable. Such a curve can be valuable in optimization tasks. For Cd, two options are curled from Figure 8a for consideration. Option A: adsorbent dosage = 0.1g, contact time = 70 min and adsorption capacity = 144.75 mg/g and Option B: absorbent dosage = 1.2g, contact time = 120 min and adsorption capacity = 7.75 mg/g. If the goal is to minimize the use of adsorbent material and contact time while still achieving effective Cd removal, the Option A is more efficient in terms of resource utilization. If the priority is to maximize the removal capacity (i.e., how much Cd can be removed), even if it requires more adsorbent and a longer contact time, then Option B may be considered optimum for achieving higher removal capacity. However, Option A demonstrates a more cost-efficient decision in this study. Using the same understanding in choosing the optimal combination in Figure 8b, 0.1 g absorbent dosage and 0.024 mg/L initial concentration will give maximum adsorption capacity of 144.75 mg/g. In Figure 8c, 0.17 mg/L initial concentration of Cd over 60 min contact time will result in 71.9999 mg/g adsorption capacity maximum values.

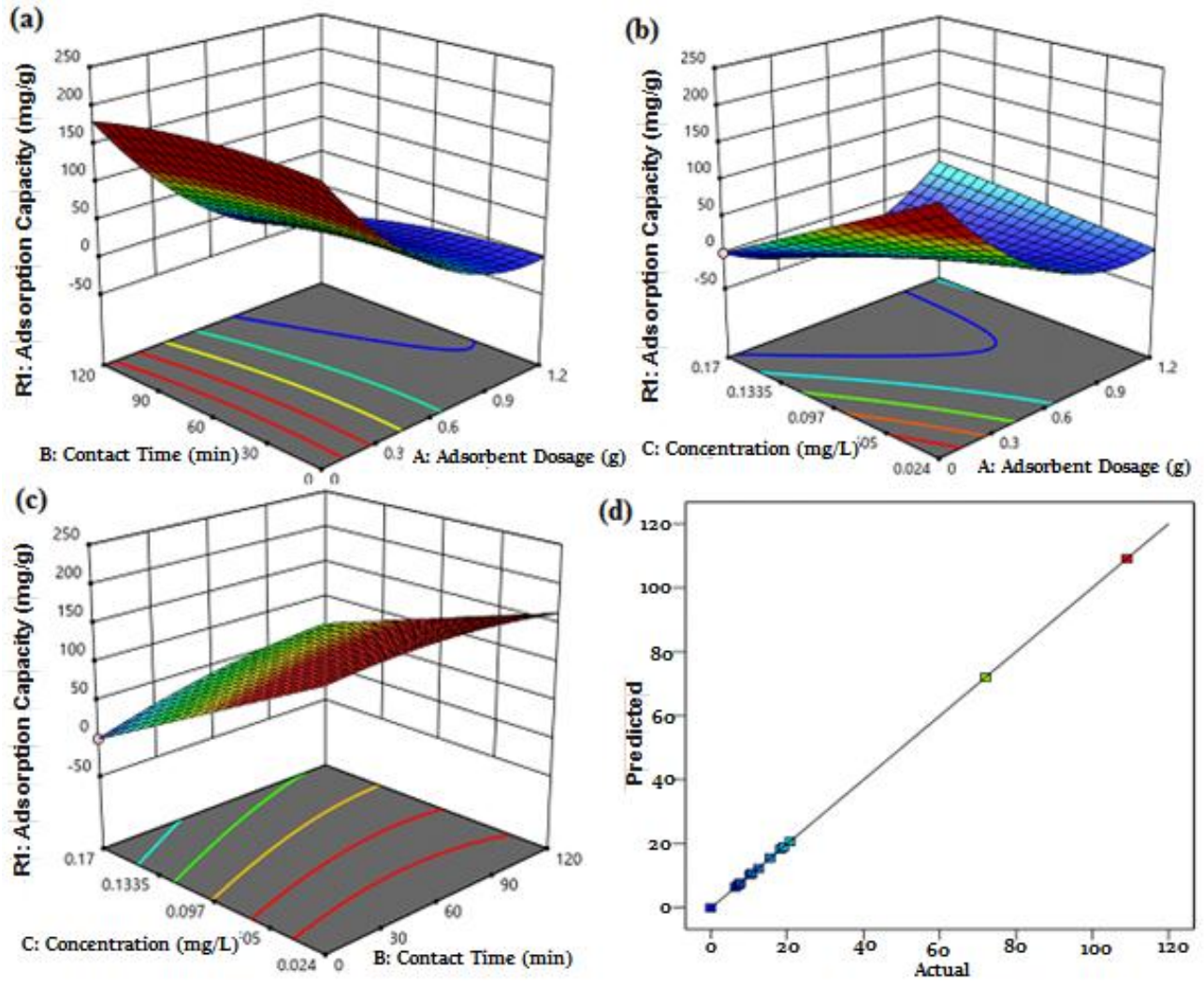

Fig. 8. R1 Against A-B, A-C & B-C and Their Observed-Predicted Values Fit.

Figure 9(a-c) highlights patterns of A-B, A-C and B-C plots versus the % removal of Cd. If categorized into 3 cases, where Case 1: optimum % removal = 85.7795%, adsorbent dosage = 0.1g and contact time = 70 min; Case 2: optimum % removal = 85.7795%, adsorbent dosage = 1.2g and initial concentration = 0.024 mg/L and; Case 3: optimum % removal = 85.7795%, initial concentration = 0.024 mg/L and contact time = 0-120 min, the following deductions can be made. Case 1 is a situation where a desired removal rate is achieved with limited adsorbent and a moderate contact time. More adsorbent is needed in Case 2 for the water containing very low initial Cd concentration to achieve the same removal rate in Case 1. As for Case 3, within a flexible time frame, the desired removal percentage can be reached regardless of the initial concentration. Since the 3 cases have identical removal percent of Cd, and in order not waste adsorbent, Case 1 and 3 optimal values may be chosen. That is, 0.1g minimal adsorbent dosage and an average of 60 min contact time, is suited to attain 85.7795% Cd removal from water containing low fraction of Cd (0.024 mg/L). Kumar et al. (2018) also combine the same 3 factors and plot a 3D surface plot based on RSM-CCD over an extended experimental time in days for Cd adsorption. Water with Cd concentration exceeding the MCL of 0.01 mg/L will cause kidney dysfunction as mentioned in Hussain et al. (2021), which is still > 0.003 mg/L (3 μg/L) WHO standard recorded in Catenacci (2014).

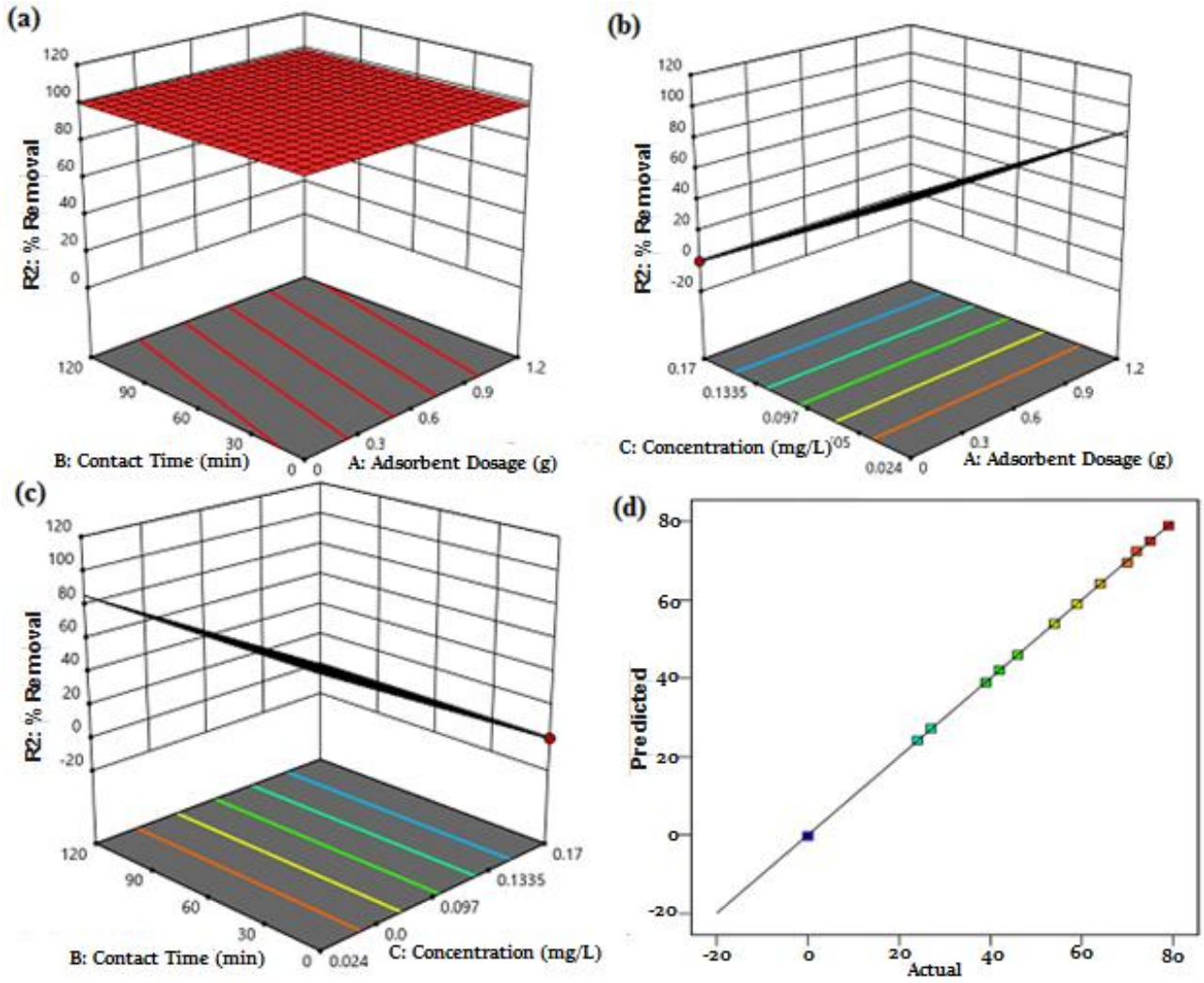

Fig. 9. R2 Against A-B, A-C & B-C and Their Observed-Predicted Values Fit.

3.3.3. Chromium

An upward-curved 3D surface plot with adsorption capacity on the z-axis, contact time on the x-axis, and adsorbent dosage on the y-axis typically represents how changes in contact time and adsorbent dosage affect the adsorption capacity of Cr or process (Figure 10a). Moving along the x-axis, the duration of water exposure to adsorbent changes, while along the y-axis, the quantity of adsorbent used changes. It is typical of Figure 10b with A & C as x- and y-axis parameters, respectively. Figure 10a starts at a peak adsorption capacity (215 mg/g), which is the highest capacity under the given condition. The fact that the plot curves downwards as we move away from the peak suggests that increasing either the contact time or adsorbent dosage beyond a certain point does not lead to higher adsorption capacity (a diminishing return effect). Hence, for maximum adsorption efficiency, the ideal or optimum combination of contact time and adsorbent dosage are 70 min and 0.1g, respectively. The curve's shape indicates that it's essential to strike a balance between contact time and adsorbent dosage to maximize efficiency while avoiding unnecessary resource consumption (e.g., excessive adsorbent usage or treatment time).

The peak (25.849 mg/g) in Figure 10b represents the maximum adsorption capacity achievable under the following experimental conditions: 0.028 mg/L C and 0.1g A. Highest adsorption capacity in Figure 10c is 199 mg/g for 0.028 mg/L initial concentration over 60 min contact period of Cr. Such a low concentration of Cr is not detrimental to human health, because it still below 50 μg/L (0.05 mg/L) WHO standard mentioned in Kapanji (2009), Karimi-Maleh et al. (2021) and Catenacci (2014). Cr in groundwater is around < 2mg/L to a skyrocketed value of around 200 mg/L according to Islam et al. (2023).

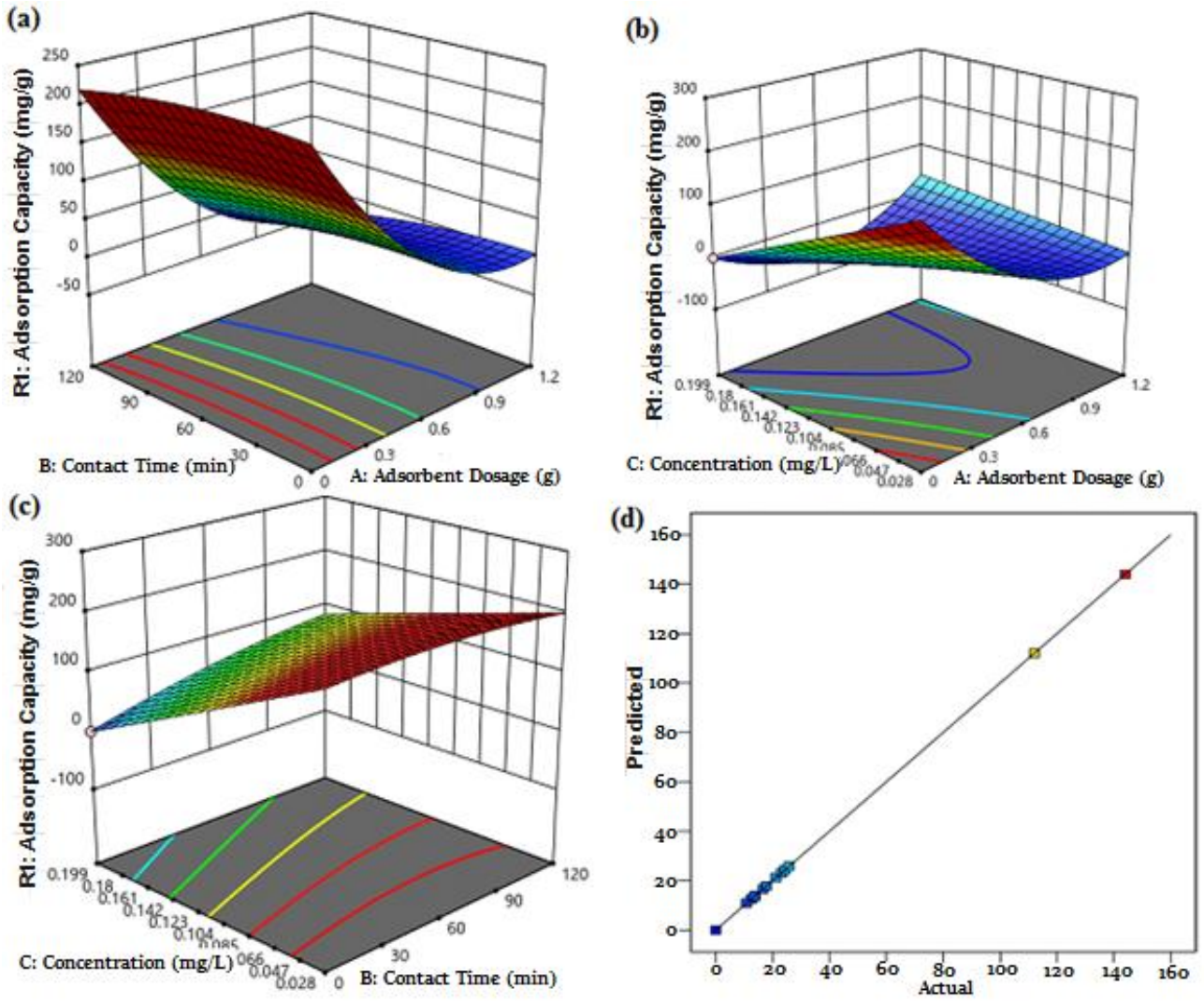

Fig. 10. 3D Surface Plots of R1 vs. A-B, A-C & B-C with Their Observed-Predicted Values Fit.

Figure 10d & 11d records perfect fit for the Cr ion removal, exceeding fits showcased by Sugashini & Begum (2013) in their work. Figure 11a proposes that the treatment process is highly effective at achieving a consistent removal rate (85.53%) under various combinations of contact time and adsorbent dosage. The flat surface provides a range of conditions (contact time from 0-120 min and adsorbent dosage from 0-1.2g) considered as the 'optimal operational zone', where a desired removal efficiency of Cr can be realized without fine-tuning the process parameters. This offers two advantages, namely, practical application and cost efficiency. The choice of specific values within this range would depend on practical considerations such as cost [27-29], resource availability, and system design constraints. Key takeaway from Figure 11a is that, there is flexibility in designing the treatment process within this range while maintaining the desired removal efficiency. According to Islam et al. (2023), grafted banana peels adsorbed 96% of Cr^{6+}, at pH = 3, 4 g/L adsorbent dose, concentration of 400 mg/L, and contact time of 120 min, making it another adsorbent of choice in lieu of watermelon rind. Under the same 85.53% removal of Cr in this study, optimal combination of initial concentration & adsorbent dosage (Figure 11b) are 0.028 mg/L & 0-1.2 g; and for the contact time and initial concentration in Figure 11c, they are 0-120 min & 0.028 mg/L respectively. But in practical sense, the contact time and the adsorbent dosage must be > 0. There may be need to reconcile the value obtained here and the optimal condition (pH = 2, initial Cr^{6+} concentration = 300 mg/L, adsorbent dosage = 0.14g, removal rate = 99.8% & 52.7 mg/g adsorption capacity) obtained by Sugashini & Begum (2013) using rice husk derivative.

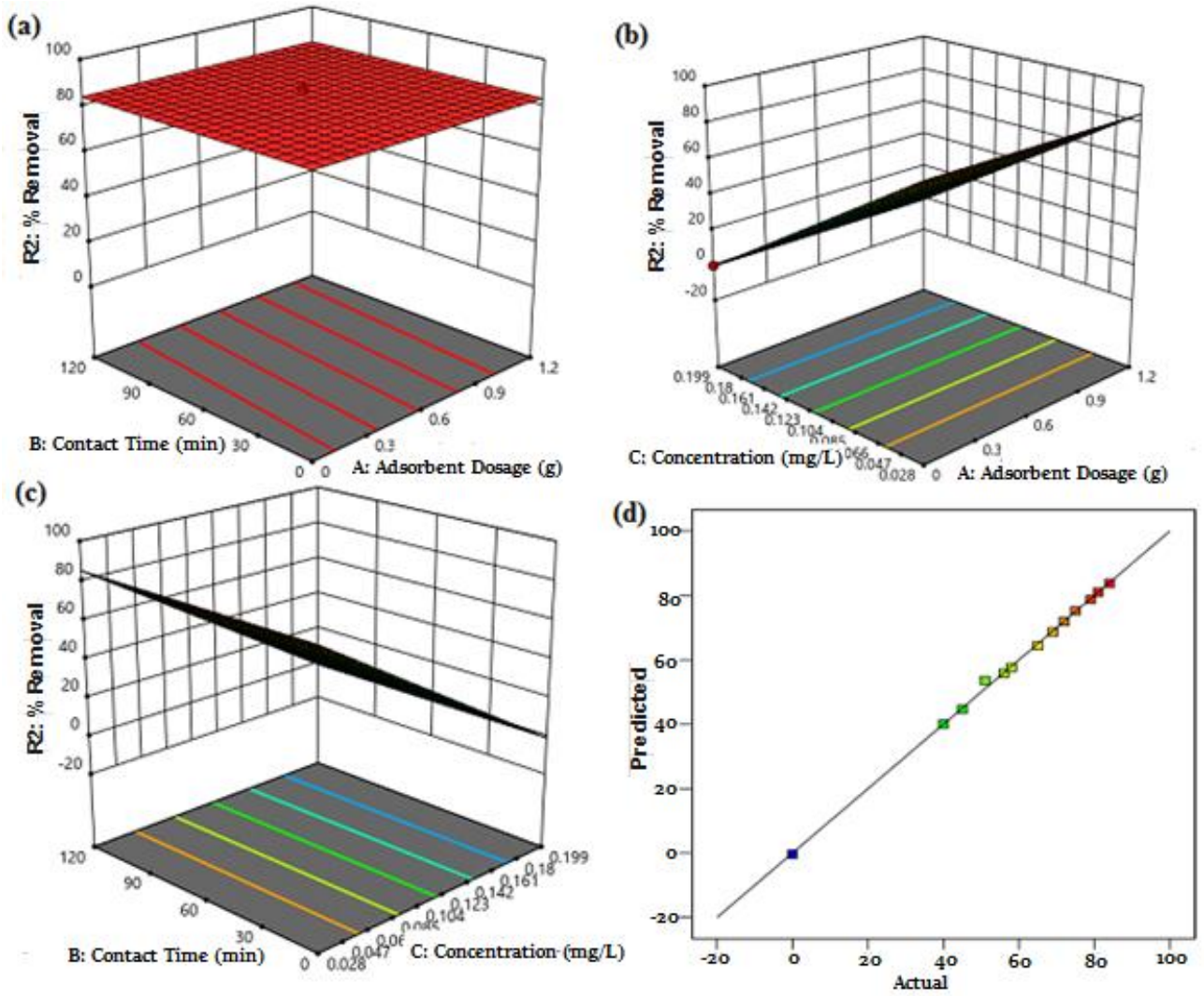

Fig. 11. 3D Surface Plots of R2 vs. A-B, A-C & B-C with Their Observed-Predicted Values Fit.

3.3.4. Copper

An upward-curved 3D surface plot with adsorption capacity on the z-axis, contact time on the x-axis, and adsorbent dosage on the y-axis (Figure 12a) commonly depicts how variations in contact time and adsorbent dose affect the adsorption capacity of Cu or process. The time of water exposure to adsorbent changes as you move along the x-axis, while the amount of adsorbent used changes as you move along the y-axis. Figure 12b's x- and y-axis parameters are A and C, respectively. Figure 12a begins with the maximum capacity (245.35 mg/g) under the given conditions. It follows a diminishing return effect as observed previously in Figure 10a. The fact that the figure trends downward as we go away from the peak shows that increasing either the contact time or adsorbent dose beyond a certain point does not result in increased adsorption capacity. As a result, for maximal adsorption effectiveness, the ideal or optimum contact duration and adsorbent dose are 120 minutes and 0.1g, respectively. The form of the curve illustrates that it is critical to achieve a balance between contact duration and adsorbent dose in order to improve efficiency while minimizing needless resource consumption. Figure 12b shows the maximal adsorption capacity attained under the following experimental conditions: 0.041 mg/L C and 0.1g A. In Figure 12c, the highest adsorption capacity for 0.041 mg/L starting concentration over 60 min contact duration of Cu is 275 mg/g.

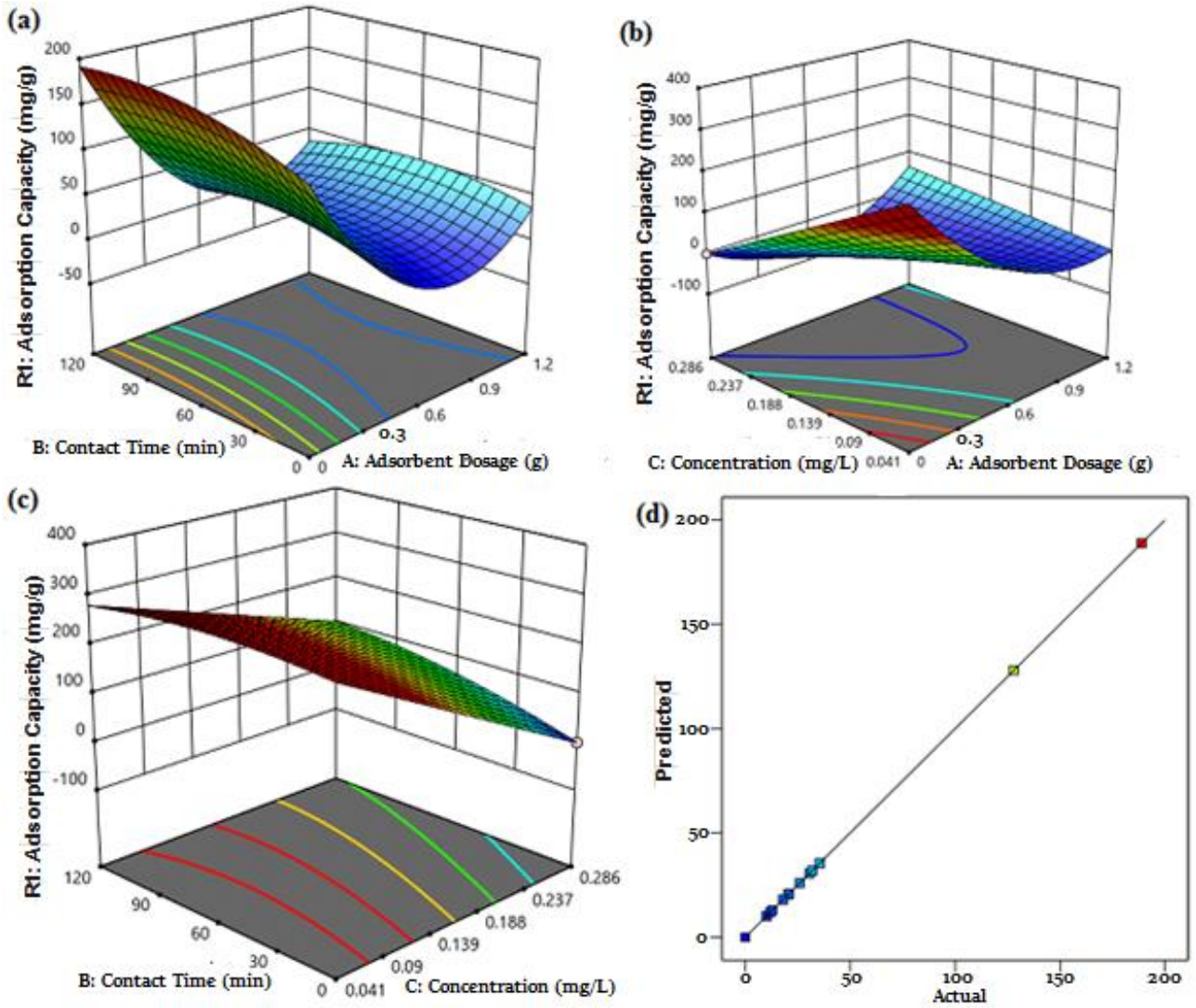

Fig. 12. Correlated Graphs of R1 Experimental and Predicted Responses and the 3D Surface Diagrams of R1 vs. A-B, A-C & B-C.

According to Figure 13a, the treatment technique is extremely successful in achieving a constant removal rate (80%) under diverse contact duration and adsorbent dose combinations. The flat surface provides a range of conditions (contact time from 0-120 min and adsorbent dosage from 0-1.2g) considered the 'optimal operational zone,' where the desired Cu removal efficiency can be realized without fine-tuning the process parameters, offering two advantages: real-world usage and cost efficacy – which is prime in adsorption processes [30]. Specific values within this range would be determined by practical factors such as cost, resource availability, and system design restrictions. Figure 13a shows that there is some leeway in planning the treatment method within this range while keeping the target removal efficiency. Under the same 80% removal of Cu, the ideal starting concentration and adsorbent dose (Figure 13b) are 0.041 mg/L & 0-1.2 g, respectively; while the contact duration and initial concentration in Figure 13c are 0-120 min & 0.041 mg/L, respectively. In practice, however, the contact period and adsorbent dose must be more than 0. Water scientist in the locality must regularly check their tap water sources to keep it at or below 2 mg/L (2000 μg/L) WHO acceptable limit reported by Catenacci (2014). Long ago, Kapanji, (2009) reported a conflicting value of 0.002 mg/L (2 μg/L) as WHO standard, which suggest that the latter is the updated record with the organization.

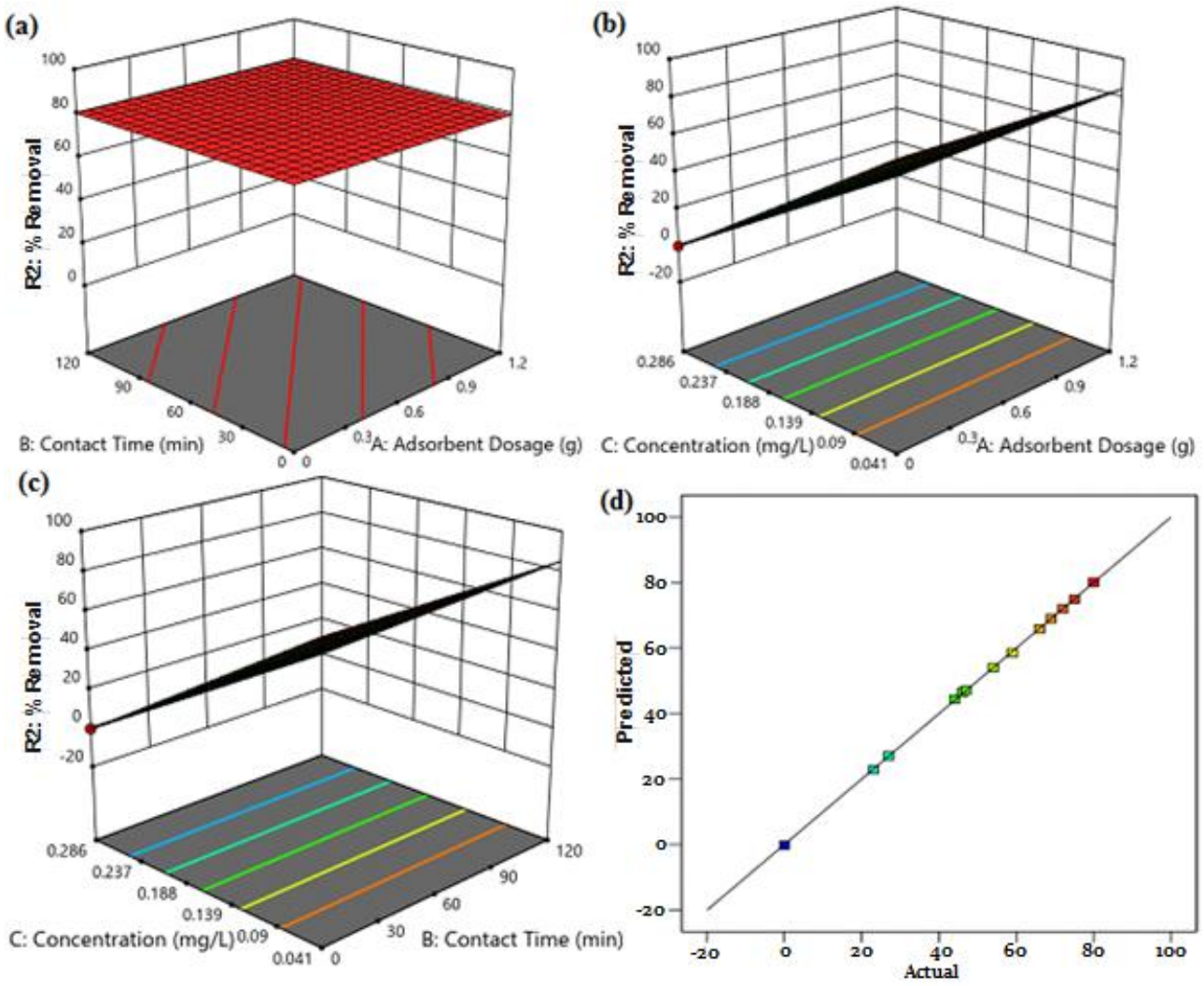

Fig. 13. Correlated Graphs of R2 Experimental and Predicted Responses and the 3D Surface Diagrams of R2 vs. A-B, A-C & B-C.

3.3.5. Lead

Previously, Yarkandi (2014)'s result show that Pb^{2+} increases with initial metal ion concentration, contact time and solution pH but decreases with amount of adsorbent and temperatures from the use of natural bentonite and activated carbon as adsorbent. The optimal adsorption capacity of Pb is 205 mg/g in Figure 14a beyond the highest value equal to 171.448 mg/g reported in Figure 5. This rise implies that optimizing the contact time and adsorbent dosage could lead to improved adsorption efficiency, making the process more effective for removing Pb from the solution. In all the 3D surface plots, the lines or contours on the inner base surface correspond to the values of the surface plot itself. These lines are contour lines or contour curves, and they represent points on the surface plot that have the same numerical value. Each contour line represents a specific constant value, allowing you to see patterns and variations in the data more easily. Hence, the peak on the z-axis of Figure 14a occurs at 0-120 min and 0.1g adsorbent dosage. Whereas in Figure 14b, 0.1g adsorbent dosage combined with 0.029 mg/L starting concentration, corresponds with 129.001 mg/g adsorption capacity of Pb in water. At 0-120 min or an average of 60 min contact time, combined with low initial concentration of 0.029 mg/L are the optimal factor that tallies with 198 mg/g Pb, as shown in Figure 14c. Pb concentration at tap, according to WHO should be 10 μg/L (0.01 mg/L) [23], implying the need for adsorption instrumentation to detoxify water from Ngomari, Maiduguri, Nigeria.

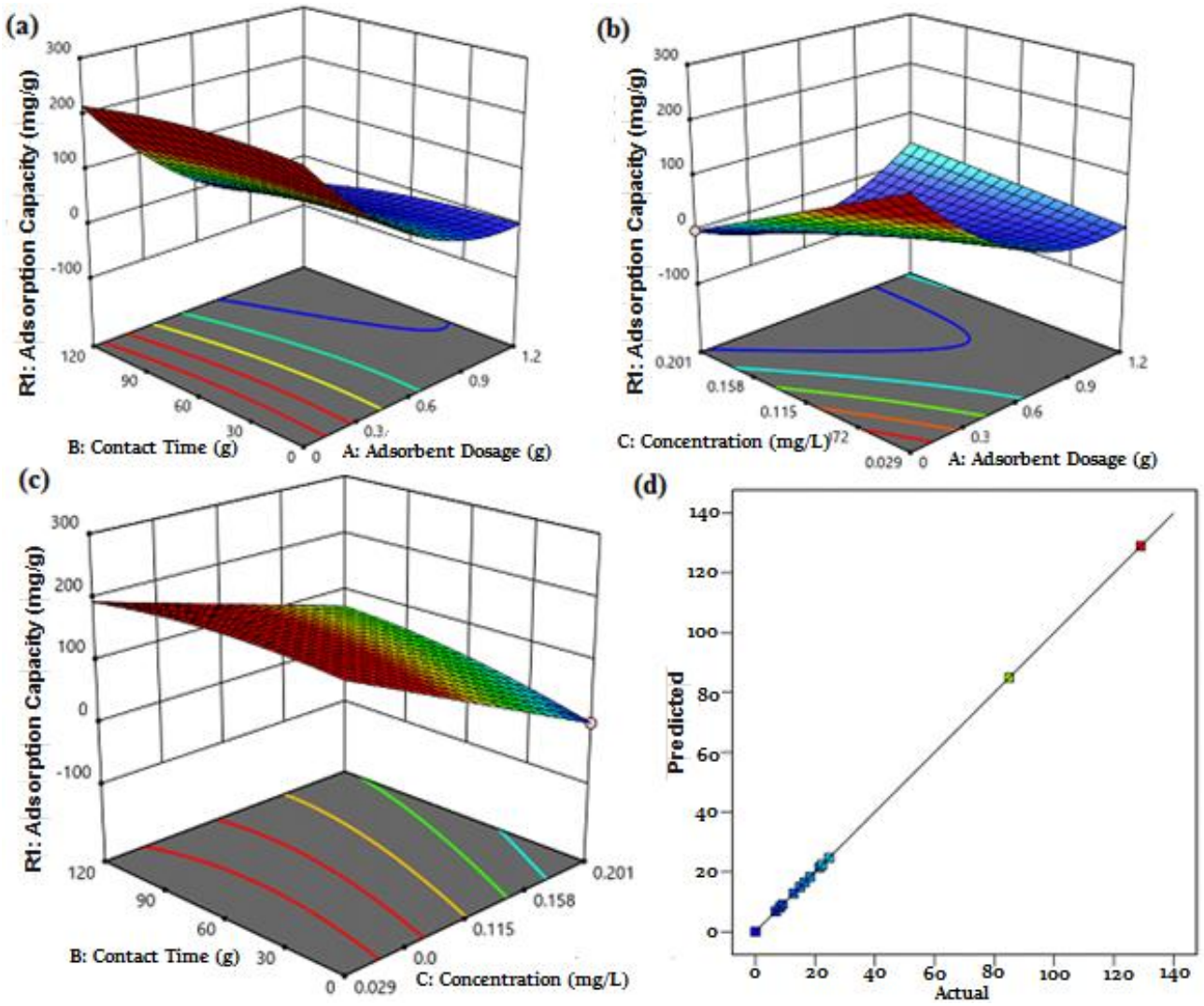

Fig. 14. 'Pb' Interrelated Graphs of R1 Experimental and Predicted Responses and the 3D Diagrams of R1 Set Against Two Possible Factor Combinations.

A slight deep at opposite ends of the somewhat plain red surface in Figure 15a describes the relationship between the % removal of Pb against adsorbent dosage and contact time. At 83.42% removal of Pb, the contact time has significant effect on the R2 based on the observed patterns on the contour lines. A non-linear relationship exists such that changing the contact times and the adsorbent dosage affects the dependent variable significantly. Their values are 0-120 min and 0.1-1.2g for the R2 reported. In Figures 15(b & c), the contour lines are parallel to the x-axis and y-axis respectively. Simply because the variable corresponding to the axis (i.e., adsorbent dosage and contact time) has little to no effect on the values of the surface plot. Specifically, changing the adsorbent dosage in Figure 15b (from 0-1.2g) and the contact time in Figure 15c (from 0-120 min) did not significantly impact the dependent variable represented by the surface plot. In both situations, a very low initial concentration of Pb (0.029 mg/L) in the water sample may be chosen. Golomeova & Zendelska (2016) reported 97.6% Pb adsorption rate using zeolite and an adsorption capacity of 0.39 mg/g for 5 mg/L initial concentration, which nearly tally with this result.

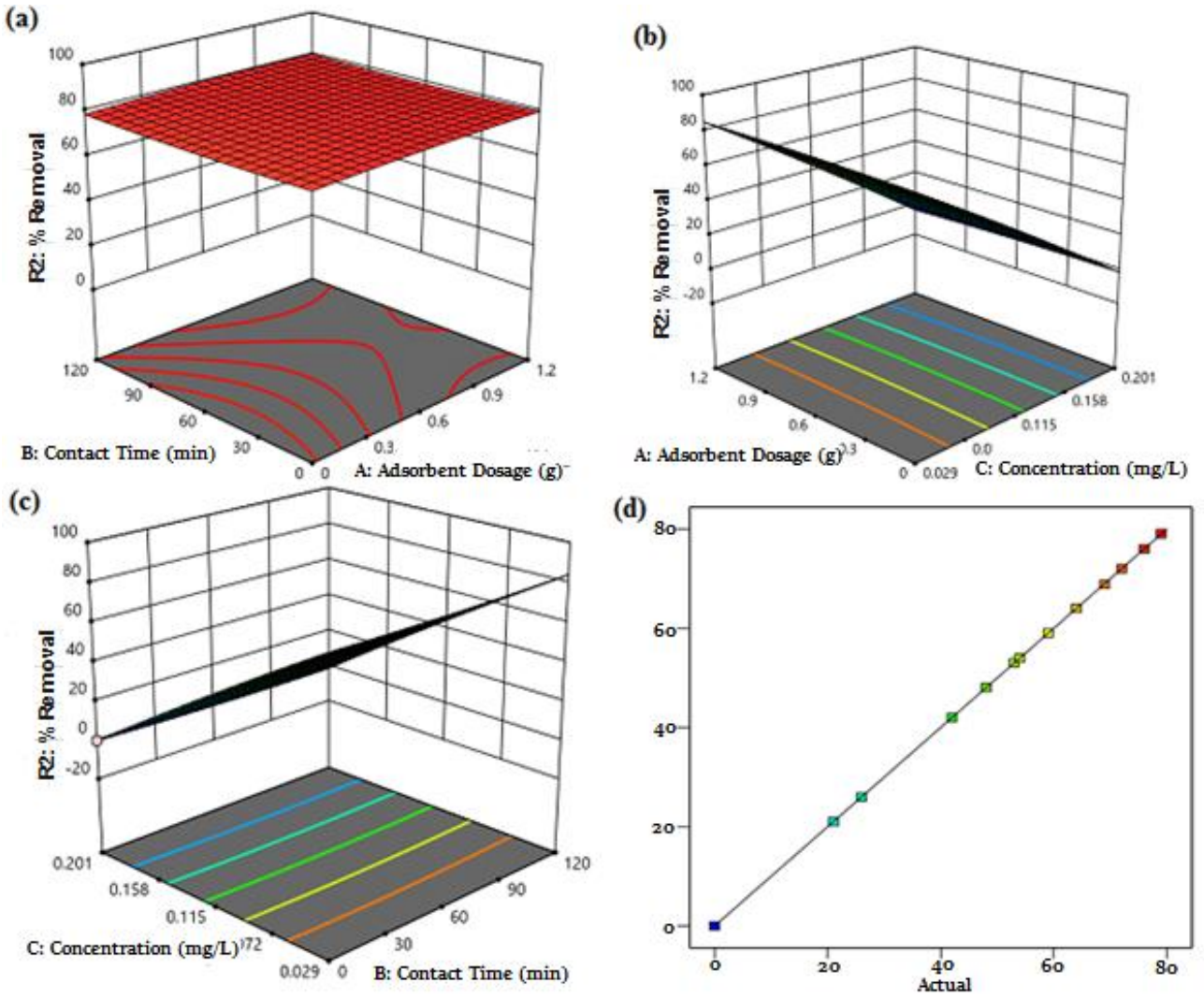

Fig. 15. 'Pb' Interrelated Graphs of R2 Experimental and Predicted Responses and the 3D Diagrams of R2 Set Against Two Possible Factor Combinations.

Values of C.V.%, R^2 (unity or proximate to unity) and the lack of fit of zeros reported in Table 1 for Figures (7-15)d 's', resulted in perfect fit of both R1 and R2 predicted and experimental data graphs. The R1 linear model developed using Stat-Ease for As was incapable of predicting the dependent variable accurately resulting in serious lack of fit, as shown in Figure 6.

4. CONCLUSION

Ten simple mathematical models for 2 responses, namely adsorption capacity (R1) and % removal (R2) of 5 heavy metals present in Ngomari Bus Stop water were developed using Stat-Ease DOE software. Equally, 5 of the models are linear and the other 5, quadratic. All except the linear model for As-R1 poorly correlates the empirical data from literature and the estimated values. The 10 models were chosen based on their lower p-values coupled with several other model performance evaluators or estimated statistical parameters for model comparison and selection such as R^2, C.V.%, AICc and BIC. Three factors, A, B & C of the models analyzed using 3D contour lines reveals the optimal combination of 2 factors with each output for all 5 heavy metals. Namely, A = 0.1g, B = 120 min & C = 0 mg/L when R1 = 3.12 mg/g and A = 1.2g, B = 120 min & C = 0 mg/L when R2 = 100% for As; A = 0.1g, B = 60 min & C = 0.17 mg/L when R1 = 144.75 mg/g and A = 0.1g, B = 60 min & C = 0.021 mg/L when R2 = 85.7795% for Cd; A = 0.1g, B = 60 min & C = 0.028 mg/L when R1 = 215 mg/g and A = 0.1-1.2g, B = 0<B≤120 min & C = 0.028 mg/L when R2 = 85.53% for Cr; A = 0.1g, B = 60 min & C = 0.041 mg/L when R1 = 275 mg/g and A = 0.1-1.2g, B = 0<B≤120 min & C = 0.041 mg/L when R2 = 80% for Cu and; A = 0.1g, B = 60 min

& C = 0.029 mg/L when R1 = 205 mg/g and A = 0.1-1.2g, B = 0<B≤120 min & C = 0.029 mg/L when R2 = 83.42% for Pb. From the forgone, a low adsorption dosage and contact time that will lead to optimum R1 and R2 should always be favoured. Better performance of the process may be further examined if adsorption isotherm models are utilized for the observations in Figures 1-5, as well as finding other models through neural network predictive modelling.

Acknowledgement

We would like to thank Mr. Muhammad Abubakar (B.Eng. Degree from University of Maiduguri, Nigeria – auwalmoh27@gmail.com) for making available his earlier research findings and on whose permission different approach was adopted in this study to analyse his findings, thereby adding to knowledge in the field of study.

REFERENCES

[1] C. C. Femina, T. Kamalesh, P. S. Kumar, and G. Rangasamy, "A critical review on the sustainable approaches from the removal of toxic heavy metals from water systems," *Ind. Eng. Chem. Res.*, vol. 62, no. 22, pp. 8575–8601, 2023, doi: 10.1021/acs.iecr.3c00709.

[2] M. S. Alhakawati, "Heavy metal removal using polymer immobilised biomass," *University of Southampton*, 2003.

[3] N. Morin-Crini et al., "Hemp-based materials for metal removal," in *Environmental Chemistry for a Sustainable World*, Springer Nature, 2018, pp. 1–34.

[4] A. Hussain, S. Madan, and R. Madan, "Removal of heavy metals from wastewater by adsorption," in *Heavy Metals - Their Environmental Impacts and Mitigation*, InTech Open, 2021, pp. 1–24.

[5] M. Golomeova and A. Zendelska, "Application of some natural porous raw materials for removal of lead and zinc from aqueous solutions," in *Microporous and Mesoporous Materials*, InTech Open, 2016, pp. 1–49.

[6] Y. A. Adamu, "Removal of heavy metals by adsorbent produced from Khaya senegalensis," *FUDMA J. Sci.*, vol. 7, no. 1, pp. 29–34, 2023, doi: 10.33003/fjs-2023-0701-1168.

[7] V. Kumar, J. Singh, and P. Kumar, "Response surface methodology based optimization of cadmium and lead remediation from aqueous solution by water hyacinth (Eichhornia crassipes [Mart.] Solms) and its anatomical study," *Arch. Agric. Environ. Sci.*, vol. 3, no. 2, pp. 163–173, 2018, doi: 10.26832/24566632.2018.0302010.

[8] S. W. Moolenaar, "Sustainable management of heavy metals in agro-ecosystems," *The Netherlands*, 1998.

[9] D. Popugaeva, "Analysis and control of aluminum concentration in groundwater: Mathematical modelling and laboratory study," *Electronic Thesis and Dissertation Repository*, 2019.

[10] S. Ababneh, O. Al-Araidah, and M. Almomani, "An analytic hierarchy process model for selecting adsorbent for heavy metal ion removal from wastewater," *Water SA*, vol. 46, no. 3, pp. 493–499, 2020, doi: 10.17159/wsa/2020.v46.i3.8659.

[11] K. K. Kapanji, "The removal of heavy metals from wastewater using South African clinoptilolite," *University of the Witwatersrand, Johannesburg*, 2009.

[12] E. M. Trujillo, T. H. Jeffers, C. Ferguson, and H. Q. Stevenson, "Mathematically modeling the removal of heavy metals from a wastewater using immobilized biomass," *Environ. Sci. Technol.*, vol. 25, no. 9, pp. 1559–1565, 1991, doi: 10.1021/es00021a005.

[13] M. Endalew, "Adsorptive removal of Cr(VI) from tannery wastewater using biochar derived from organic fraction of municipal solid waste," *College of Health Sciences, Jimma University, Jimma, Ethiopia*, 2016.

[14] J. Bayuo, K. M. Mtei, M. Sillanpaa, and K. M. Mtei, "Removal of heavy metals from binary and multicomponent adsorption systems using various adsorbents – a systematic review," *RSC Adv.*, vol. 13, pp. 13052–13093, 2023, doi: 10.1039/D3RA01660A.

[15] S. Mzimela, "The biosorption of chromium and copper from AMD contaminated water using banana peels as a biomass adsorbent," *Durban University of Technology*, 2022.

[16] N. H. Yarkandi, "Removal of lead (II) from wastewater by adsorption," *Int. J. Curr. Microbiol. Appl. Sci.*, vol. 3, no. 4, pp. 207–228, 2014, [Online]. Available: http://www.ijcmas.com/vol-3-4/Naeema%25...

[17] O.-A. O. Abiodun et al., "Remediation of heavy metals using biomass-based adsorbents: Adsorption kinetics and isotherm models," *Clean Technol.*, vol. 5, pp. 934–960, 2023, doi: 10.3390/ cleantechnol5030047.

[18] V. R. Fanaie, M. Karrabi, M. M. Amin, B. Shahnavaz, and A. Fatehizadeh, "Application of response surface methodology and artificial neural network for analysis of p-chlorophenol biosorption by dried activated sludge," *J. Appl. Chem. Res.*, vol. 10, no. 2, pp. 25–37, 2016, [Online]. Available: www.jacr.kiau.ac.ir.

[19] B. R. Poudel, "Adsorptive removal of metallic and non-metallic pollutants from water by chemically modified natural ion exchanger," *Institute of Science and Technology, Tribhuvan University Nepal*, 2022.

[20] S. Sugashini and K. M. M. S. Begum, "Column adsorption studies for the removal of Cr (VI) ions by ethylamine modified chitosan carbonized rice husk composite beads with modelling and optimization," *J. of Chemistry*, vol. 2013, no. 460971, pp. 1–11, 2013, doi: 10.1155/2013/460971.

[21] O. O. Ogunleye, M. A. Ajala, S. E. Agarry, and O. O. Agdebe, "Experimental optimization of lead (II) bioadsorption from aqueous solution onto banana stalk using central composite design," *Chem. Mater. Res.*, vol. 7, no. 11, pp. 35–49, 2015, [Online]. Available: www.iiste.org.

[22] H. A. Atta, K. K. Hummadi, and M. J. M-Ridha, "The application of response surface methodology and Design-Expert® for analysis of ciprofloxacin removal from aqueous solution using raw rice husk: Kinetic and isotherm studies," *Desalin. Water Treat.*, vol. 248, pp. 203–216, 2022, doi: 10.5004/dwt.2022.28074.

[23] A. Catenacci, "Heavy metal removal from water: Characterization and applicability of unconventional media," *PhD School of Politecnico di Milano Doctoral*, 2014.

[24] H. de-G. Acquah, "Comparison of Akaike information criterion (AIC) and Bayesian information criterion (BIC) in selection of an asymmertic price relationship," *J. Dev. abd Agric. Econ.*, vol. 2, no. 1, pp. 001–006, 2010, [Online]. Available: http://www.academicjournals.org/JDAE.

[25] L. M. Collins, J. J. Dziak, and R. Li, "Design of experiments with multiple independent variables: A resource management perspective on complete and reduced factorial designs," *Psychol Methods*, vol. 14, no. 3, pp. 202–224, 2009, doi: 10.1037/a0015826.

[26] S. M. Sanchez and H. Wan, "Better than a petaflop: The power of efficient experimental design," in *Proceedings of the 2009 Winter Simulation Conference*, 2009, pp. 60–74, doi: 10.1109/WSC.2008.4736057.

[27] H. Karimi-Maleh et al., "Recent advances in removal techniques of Cr(VI) toxic ion from aqueous solution: A comprehensive review," *J. Mol. Liq.*, vol. 329, no. 115062, 2021, doi: 10.1016/J.MOLLIQ.2020.115062.

[28] M. Islam, A. A. Mohana, A. Rahman, M. Rahman, R. Naidu, and M. M. Rahman, "A comprehensive review of the current progress of chromium removal methods from aqueous solution," *Toxics*, vol. 11, no. 252, pp. 1–43, 2023, doi: 10.3390/ toxics11030252.

[29] E. T. Musapatika, "Use of low cost adsorbents to treat industrial wastewater," *University of the Witwatersrand, Johannesburg*, 2010.

[30] A.-E. Segneanu, R. Trusca, C. Cepan, M. Mihailescu, C. Muntean, and I. Grozescu, "Innovative low-cost engineered adsorbents based on waste eggshell for nickel removal from aqueous solutions," *Res. Sq.*, pp. 1–35, 2023, doi: 10.21203/rs.3.rs-2613416/v1.